

Calcium-Looping performance of mechanically modified Al₂O₃-CaO composites for energy storage and CO₂ capture

Monica Benitez-Guerrero^{1, 2}, *Jose Manuel Valverde*^{1*}, *Pedro E. Sanchez-Jimenez*²,
Antonio Perejon^{2, 3}, *Luis A. Perez-Maqueda*².

¹ Facultad de Física, Universidad de Sevilla, Avenida Reina Mercedes s/n, 41012 Sevilla, Spain.

² Instituto de Ciencia de Materiales de Sevilla, C.S.I.C.-Universidad de Sevilla, C. Américo Vespucio nº49, 41092 Sevilla, Spain.

³ Facultad de Química, Universidad de Sevilla, Avenida Reina Mercedes s/n, 41012 Sevilla Spain

*Prof. Dr. J.M. Valverde

Facultad de Física

Universidad de Sevilla

Avenida Reina Mercedes s/n, 41012 Sevilla (Spain)

Tel +34 954550960 Fax +34 954239434

E-mail: jmillan@us.es

Calcium-Looping performance of mechanically modified Al₂O₃-CaO composites for energy storage and CO₂ capture

Highlights:

- * Al₂O₃/limestone composites were prepared by ball milling with Al₂O₃ contents in the range between 5 and 20%wt
- * The composites were subjected to calcination-carbonation cycles at conditions for CO₂ capture and energy storage
- * Diverse types of calcium aluminate were formed as depending on the Calcium Looping conditions.
- * High Al-content leads to deactivation mainly by the formation of Ca₃Al₂O₆ at CO₂ capture conditions
- * At energy storage conditions, the residual effective conversion of the composites is twice that of limestone

Abstract:

This work reports the Calcium-Looping (CaL) multicycle performance under energy storage and CO₂ capture conditions of different Al-composites prepared by milling mixtures of nanoalumina and natural limestone powders. The micro- and nanostructure of the composites has been analyzed by X-ray diffraction, scanning electron microscopy and high-resolution transmission electron microscopy as affected by the type of CaL conditions employed, either for energy storage in Concentrated Solar Power (CSP) plants or for post-combustion CO₂ capture. Two types of calcium aluminates are formed under these diverse CaL conditions. A calcium aluminate with ratio Ca/Al < 1 (Ca₄Al₆O₁₃) is formed under CaL-CSP conditions, which helps stabilize the CaO microstructure and mitigate pore-plugging. On the other hand, a crystalline phase Ca₃Al₂O₆ is formed (Ca/Al > 1) under CaL-CO₂ capture conditions presumably due to the higher calcination temperature, which withdraws from the sorbent a relatively high amount of active Ca. Moreover, the addition of nano-alumina, and the consequent generation of calcium aluminates, affects in diverse ways the microstructure and morphology of the CaO particles as depending on the CaL application, which critically modifies the performance of the composites.

Keywords: Calcium Looping; Energy Storage; CO₂ capture; Concentrated Solar Power; Al-Ca composites

1. Introduction

The Calcium-Looping (CaL) process is at the basis of a 2nd generation CO₂ capture technology for removing CO₂ from post-combustion gases already demonstrated at large pilot scale (1-2 MWth) [1-5]. The process relies upon the reversible carbonation/calcination reaction of CaO



Carbonation takes place at temperatures around ~ 650 °C in a fluidized bed reactor where the post-combustion flue gas carries a CO₂ concentration close to 15 vol% at atmospheric pressure. After carbonation, CaCO₃ particles are circulated into a second reactor (calciner) where calcination, under necessarily high CO₂ concentration and high temperature (~ 930-950°C), regenerates the CaO particles [6, 7]. Once CaO particles are regenerated, they are recirculated into the carbonator for a subsequent new cycle. The CO₂ extracted from the calciner at high concentration can be thus compressed and stored or employed in other uses. This process is schematized in Figure 1a.

In the last years, the CaL process has acquired a renewed interest for Thermochemical Energy Storage (TCES) in Concentrated Solar Power (CSP) plants [8-11]. The CaO/CaCO₃ system offers a high energy storage density (about 3.26 GJ/m³) which would allow electricity generation in CSP plants on demand overcoming the issues derived from the variable nature of direct solar irradiation [12, 13]. A detailed CaL-CSP energy integration scheme has been recently proposed by Chacartegui et al. [13]. Basically, the integrated system consists of a solar calciner, a carbonator, a CO₂ compression-storage system, two tanks for CaO and CaCO₃ storage and a Brayton-based power unit (Figure 1b) [13, 14]. Thus, the endothermic calcination reaction takes place when direct solar irradiation is available, which serves to store the excess heat as chemical energy, whereas the exothermic carbonation reaction is carried out at night or during limited solar activity, which releases heat to be carried by the CO₂ in excess to the power block. The use of Helium gas in the calciner in a closed cycle helps reduce the calcination temperature in short residence times to about 700 °C [15] due to the enhancement of the thermal conductivity and CO₂ diffusivity in He [16, 17]. The He/CO₂ mixture could be separated by selective membranes [18], allowing the storage and recirculation of the gases individually in both closed cycles.

The low price, wide availability and non-toxicity of natural Ca-based materials such as limestone, makes the CaL process very interesting for large-scale applications such as CO₂ capture and energy storage [19-23]. However, most of natural Ca-based materials exhibit a progressive deactivation as the number of carbonation/calcination cycles is increased, which is particularly marked at CO₂ capture conditions [6, 24, 25]. Thus, cost-effective treatments are being investigated to enhance the CaO multicycle stability such as thermal activation [26-29], hydration [29-31] and mechanical activation or milling [32-34]. An alternative strategy consists of the synthesis of composites through the controlled addition of inert materials with high Tamman temperature to stabilize the CaO structure [20, 21, 35]. Thus, the performance of Al-containing sorbents has been widely investigated at diverse CaL conditions [35-39]. Florin et al. [40] employed a coprecipitation method by bubbling CO₂ through an aqueous solution containing Ca(OH)₂ and Al(NO₃)₃ for the synthesis of Ca-based materials with different

contents of mayenite ($\text{Ca}_{12}\text{Al}_{14}\text{O}_{33}$) after calcination at 800 °C. These authors found that the capture capacity of the composites increased as the binder aluminate content was increased. However, a proportion of $\text{Ca}_{12}\text{Al}_{14}\text{O}_{33}$ higher than 15 wt% yielded a decrease of the CO_2 capture capacity and hampered the mechanical stability of the composite. By means of a sol-gel method, Broda et al. [35, 37] synthesized gels with $\text{Ca}^{2+}/\text{Al}^{3+}$ molar ratios from 90/10 to 50/50, using aluminum isopropoxide and different Ca sources. After calcination at 800 °C for 2 hours a small amount of $\text{Ca}_{12}\text{Al}_{14}\text{O}_{33}$ was also formed. The results obtained from CO_2 capture multicycle tests indicated that the composite with higher activity had a Ca/Al molar ratio of 90/10. Recently, Sun et al. [33] analyzed the effect of the addition of gibbsite ($\text{Al}(\text{OH})_3$, 5-40%) to natural limestone after milling using a planetary ball mill. They concluded that, despite the formation of $\text{Ca}_3\text{Al}_2\text{O}_6$ binder, the addition of Al did not yield clear benefits. However, grinding limestone did enhanced the CO_2 capture performance.

In recent years, the use of Ca/Al composites has been analyzed for thermochemical energy storage in CSP plants based either on the $\text{CaO}/\text{Ca}(\text{OH})_2$ system [22] or CaO/CaCO_3 [41] for the storage of medium and high temperature heat, respectively. Sakellariou et al. [41] have analyzed the calcination/carbonation behavior of Ca/Al composites prepared from calcium and aluminum nitrates with different Ca/Al molar ratios (95/5, 80/20 and 52/48) following the modified Pechini route and calcining at 900 °C for 2h under air atmosphere. They showed that the most effective compound (80/20 Ca/Al) exhibited a high surface area and a significant amount of $\text{Ca}_3\text{Al}_2\text{O}_6$ binder. However, an excessive formation of calcium aluminate caused a premature deactivation as was the case of the composite with the molar ratio of 52/48. In the same line, Obermeier et al. [42] synthesized different Al-composites (Ca/Al molar ratios of 95/5, 90/10, 80/20 and 75/25) from Ca-citrate and Al-nitrate, and analyzed their multicycle performance under CaL-CSP conditions introducing of a steam hydration stage at different temperatures. The results indicated that neither the temperature increase nor the presence of water vapor had a significant effect on the CaO performance.

Notwithstanding the different methodologies employed to synthesize Al-modified CaO sorbents, a simpler and cost effective method for producing large amounts of sorbent is needed. Just physical mixing and milling of natural limestone and Al-based compounds is a cost-effective technique poorly investigated for CO_2 capture [33] and, to our knowledge, unexplored yet for energy storage. The present work analyzes and compares for the first time the CaL multicycle performance under energy storage and CO_2 capture conditions of different composites prepared by milling powdered nanoalumina and limestone at different proportions. The research includes the analysis of the micro- and nanostructure of the composites by X-ray diffraction, scanning electron microscopy and high resolution transmission electron microscopy. As will be seen, two distinct types of calcium aluminate are formed as depending on the type of CaL conditions used which, in addition to microstructural effects, helps explain the diverse behaviors exhibited by the alumina composites as depending on the type of CaL conditions.

2. Materials and Methods

A high-purity limestone was employed in the present work from Taljedi quarry (Sevilla, Spain) (99.4% wt CaCO_3 , with a small proportion of impurities such as 0.09% wt Al_2O_3 , 0.09%

wt Fe₂O₃, 0.02%wt K₂O, 0.17% wt MgO, 0.17% wt SiO₂, 0.02% wt P₂O₅ and 0.02% wt SO₃). After sieving, the fraction above 160 μm was selected for the study.

The aluminum oxide nanopowder (Al content > 99.8%, supplied by Strem Chemicals) used as additive in this work is a quasi-amorphous alumina formed by the transition aluminas χ -Al₂O₃ (PDF card 13-0373) and γ -Al₂O₃ (PDF card 10-0425) (Fig. 2a). The alumina particles are mainly hexagonal platelets (Fig. 2b) of size between 0.3 and 5 μm, peaking at 1.65 μm (Fig. 2c). Surface area and granulometric data measured for the nanoalumina powder employed are collected in Table 1.

Mixtures of different nanoalumina content (5, 10 and 20 wt%) and limestone were prepared. In order to obtain homogeneous blends, the samples were milled at 1500 rpm during 90 s in an EMAX mill (Retsch) using stainless steel jars with 50 balls (10 mm diameter), a sample mass to balls mass fraction 1/20 and a 10 g sample. The as-synthesized alumina composites were named as **5wt Al₂O₃**, **10wt Al₂O₃** and **20wt Al₂O₃**. The CaCO₃ crystallite size was decreased to a minimum value (around 20 nm) for a grinding time of 90 s that remained the same for longer grinding periods.

Multicycle CaL tests were performed using a TA instrument Q5000IR thermogravimetric analyzer, which is provided with a high sensitive balance (< 0.1 μm) and a furnace heated by IR halogen lamps. IR heating allows high heating and cooling rates (up to 300 °C/min) as well as stable isotherms. Fast heating/cooling rates are necessary to mimic realistic conditions since the material is circulated between reactors at different temperatures. All samples were tested under the following energy storage (CaL-CSP) and CO₂ capture (CaL-CO₂) conditions. The CaL-CSP experiments were started with a precalcination stage from room temperature to the calcination temperature (725 °C) at 300 °C/min under He atmosphere, and the isotherm was maintained during 5 min. Then, the carbonation step was initiated under pure CO₂, increasing the temperature (at 300 °C/min) up to 850°C, which was kept fixed for 5 min. Carbonation was followed by the calcination step under He through a quick temperature reduction (at 300 °C/min) down to 725°C, which was held for 5 min. An intermediate step was introduced after calcination by quickly decreasing the temperature to 300 °C, which was kept fixed for 2 min under He. This cooling stage was intended to replicate the extraction of sensible heat of the solids after calcination and before storage as would be the case in the practical application [13]. After this cooling stage a new cycle was started for a total of 20 carbonation/calcination cycles. These conditions were selected according to the CaL-CSP integration scheme proposed by Chacartegui et al. [13] and were used also in previous works [15, 23, 43]. Multicycle CaL-CO₂ capture experiments were started by a calcination step from room temperature to 900 °C (at 300 °C/min, held for 5 min) under high CO₂ concentration (70% CO₂/ 30% air vol/vol) at atmospheric pressure. Precalcination was followed by a carbonation stage by quickly decreasing the temperature to 650 °C at 300 °C/min, which was held for 5 min under 15% CO₂/ 85% air vol/vol. A total of 20 carbonation/calcination cycles were also run. In all runs, a small mass (10 mg) was used for avoiding undesired effects related to CO₂ diffusion resistance across the bulk.

Particle size distributions (PSDs) were measured by laser diffraction analysis using a Mastersizer 2000 equipment (Malvern). For this purpose, the samples were previously dispersed in 2-propanol and sonicated for 30 s to loosen particle aggregates.

XRD powder measurements were carried out using a MiniFlex600 (Rigaku) with Ni filtered CuK α radiation ($\lambda = 1.5406 \text{ \AA}$) at 40 kV/15 mA for a scan range $2\theta=5-90^\circ$ and a scan speed of $3^\circ/\text{min}$. Crystallite size was estimated using the PDXL2 Rigaku data analysis software.

Nitrogen adsorption-desorption isotherms were measured at 77 K (-196 °C) by employing a ASAP2420 (Micromeritics) instrument. Prior to the analysis, the samples were degassed at 350 °C for 7 h. Total surface areas (S_{BET}) were determined using the BET equation [44]. Total pore volumes (V_{sp}) were calculated from the amount of N₂ adsorbed at a P/P_0 value of 0.99.

SEM micrographs of previously gold-sputtered samples were acquired using a Hitachi S4800 FEG microscope. HRTEM micrographs and high-angle annular dark-field scanning transmission electron micrographs (HAADF-STEM) were registered using a Talos F200S FEG microscope (FEI). For this purpose the powder samples were deposited on copper grids.

Table 1: CaCO₃ crystallite size (L, estimated using the main reflection peak (104) $2\theta = 29.5^\circ$), PSD and porosimetry data for nanoalumina, milled limestone/alumina mixtures.

	L (nm)	PSDs data (μm)			S_{BET} (m^2/g)	V_{p} (cm^3/g)
		Dv(10) ^a	Dv(50) ^b	Dv(90) ^c		
Al₂O₃	Amorphous	0.9	1.7	2.9	271	0.24
Milled samples						
0wt Al₂O₃	20	1.0	6.2	72	5	0.017
5wt Al₂O₃	23	0.9	4.0	46	16	0.027
10wt Al₂O₃	19	1.0	7.4	56	23	0.038
20wt Al₂O₃	20	1.0	6.6	52	39	0.050

a Particle size limit below which 10% of the particles are found

b Mass Median Diameter (MMD).

c Particle size limit below which 90% of the particles are found

3. Results and Discussion

Figure 3 shows the PSDs and representative SEM micrographs of the different composites prepared. As seen above (Table 1), the specific surface area and pore volume are progressively increased as the Al₂O₃ content is increased (Table 1). However, Figure 3 shows that particle morphology and size distribution are rather independent of the Al₂O₃ content. A bimodal distribution is observed in Fig. 3a, peaking at 1.6 and 18 μm . Additionally, a small proportion of larger aggregates, ranging from 200 to 800 μm , is observed. These agglomerates

could be generated by incomplete grinding or by cold welding of particles as reported in ball milling studies [45, 46].

3.1) Calcium Looping (CaL) Multicycle Activity

The effective conversion $X_{ef N}$ was the parameter utilized to evaluate the samples performances when subjected to multicycle CaL tests. $X_{ef N}$ is defined as the ratio of the CaO mass converted in the carbonation stage of each N-cycle to the total sample mass before carbonation

$$X_{ef N} = \frac{m_{Carb N} - m_N}{m_N} \cdot \frac{W_{CaO}}{W_{CO_2}} \quad (2)$$

where m_N and $m_{Carb N}$ are the sample masses before and after carbonation at the Nth-cycle and W_{CaO} , W_{CO_2} are the molar masses of CaO and CO₂, respectively. The effective conversion takes into account the presence of inert compounds in the composites by using the total sample mass $X_{ef N}$. Consequently, the specific energy released in the carbonation stage per unit mass would be given by X_{ef} times ($\Delta H_r^0 / W_{CaO}$) (kJ/g), where ΔH_r^0 is the reaction enthalpy (-178 kJ mol⁻¹).

Data on the effective conversion measured for the different composites under energy storage and CO₂ capture conditions are shown in Figure 4. These data can be well fitted by the semi-empirical equation [47-49]:

$$X_{ef N} = X_{ef r} + \frac{X_1}{k(N-1) + (1 - X_r/X_1)^{-1}} \quad (3)$$

where N is the cycle number, k is the deactivation rate constant, X_1 is CaO conversion in the first cycle and $X_{ef r}$ is the residual conversion towards which conversion will converge asymptotically after a very large number of cycles. Best fitting parameters k and $X_{ef r}$ are collected in Table 2.

For comparison, data measured for the starting limestone are also included in Fig. 4. In general, it is observed that under CaL-CSP storage conditions (Fig. 4a) the multicycle effective conversions measured for the different samples are much higher than those obtained under CaL-CO₂ capture conditions (Fig. 4b). This is explained by the harsh calcination conditions used in CO₂ capture (high partial pressure of CO₂ and high temperature), which enhances CaO sintering as widely reported in previous works [6, 25, 50, 51] leading to a marked deactivation with the number of cycles. Moreover, the kinetics of carbonation is also remarkably affected by the type of conditions as Figure 5 illustrates. As well-known from previous studies [52, 53] carbonation takes place first through a fast reaction controlled phase on the free surface of the CaO particles, which is followed by a slower phase governed by the counter-current diffusion of CO₃²⁻ and O²⁻ anions across the carbonate product layer [54, 55]. As may be seen in Figure 5, carbonation in the fast reaction controlled phase is the major contribution to CO₂ uptake under CaL-CSP storage conditions. At these conditions carbonation in the solid-state diffusion phase is negligible whereas the fast reaction phase is enhanced by the high CO₂

partial pressure and high temperature used for carbonation. In contrast, carbonation in the solid-state diffusion controlled phase is relatively promoted under CO₂ capture conditions as reported in previous works [43]. The low CO₂ concentration (15% vol/vol) and lower carbonation temperature hinders the reaction kinetics while enhanced CaO sintering limits the maximum CO₂ uptake in this phase. CaL-CO₂ capture conditions lead also to the formation of a relatively thinner layer of CaCO₃ on the surface of the particles (between 40 a 60 nm) [53] as compared to carbonation conditions for CaL-CSP storage (~100 nm) [56], which would favor solid-state diffusion in the former case. As demonstrated in recent process simulation studies [57], this information on the carbonation kinetics is relevant to infer optimum values for important operation parameters such as the solids residence time in the carbonator.

Table 2. Best fitting parameters of Eq (3) to effective conversion experimental data for the composites and limestone samples tested under CaL-CSP storage and CaL-CO₂ capture conditions.

	CaL- CSP storage conditions			CaL-CO ₂ capture conditions		
	X_{efr}	k	R^2	X_{efr}	k	R^2
Raw Limestone	0.10	0.40	0.991	0.065	0.43	0.999
Milled samples						
0wt Al₂O₃	0.16	0.09	0.999	0.082	0.35	0.999
5wt Al₂O₃	0.33	0.10	0.999	0.097	0.40	0.999
10wt Al₂O₃	0.35	0.19	0.998	0.073	0.29	0.997
20wt Al₂O₃	0.36	0.64	0.999	0.039	0.31	0.999

As can be seen in Fig 4, the effects of nanoalumina addition and milling are critically dependent on the type of CaL conditions employed. Thus, limestone milling yields a remarkable improvement of the multicycle activity under energy storage conditions (Fig. 4a). This could be explained by the decrease of particle size, which minimizes deactivation by pore-plugging. As reported in previous works, pore plugging is the main limiting mechanism under CaL-CSP conditions [23]. Comparatively, the beneficial effect of milling becomes weaker under CO₂ capture conditions (Fig. 4b). Under these conditions, enhanced sintering, caused by the harsh calcination conditions (high temperature and CO₂ concentration), is the main limiting mechanism and is not greatly affected by milling [34].

The addition of nanoalumina reduces initially the effective conversion in the first cycles due to the irreversible formation of calcium aluminates (as will be seen ahead in detail), which decreases the fraction of CaO available for carbonation. However, In the case of CaL-CSP conditions, the deactivation rate is notably reduced for the Al-composites as compared to the milled limestone alone (0wt Al₂O₃), and the residual effective conversion is substantially increased to a similar value for all the composites tested ($X_{efr} \approx 0.35$), which is about twice that of milled limestone (Table 2). On the other hand, the beneficial effect of alumina addition is limited under CO₂ capture conditions to the 5wt Al₂O₃ milled composite. Under these conditions, a high alumina contents adversely affects the activity of the composite. In

accordance with previous reports [33, 58], an excessive Al_2O_3 content produces a decrease of the CO_2 uptake simply due to the considerable reduction of the active phase CaO. Furthermore, some authors have pointed out that the incorporation of Al^{3+} aliovalent ions may add lattice defects in sorbent crystals that would promote sintering of the CaO grains [59].

Under both type of CaL conditions, the 5wt Al_2O_3 milled composite exhibits the best performance along the 20 cycles tested. To further analyze this point, Figure 6 shows the relative variation of X_{ef} for this composite with respect to limestone milled alone. As can be seen, the relative improvement of performance for this composite is increased with the number of cycles under CaL-CSP storage conditions whereas it remains more or less stable from the first cycle under CO_2 capture conditions. This different behavior is explained by the diverse formation of calcium aluminates in both cases as described hereafter.

The effectiveness of the simple milling method employed in the present work can be further appreciated by a comparison of the performance of the 5%wt Al_2O_3 composite with that of other composites of similar composition but synthesized through more complex routes. Thus, our composite exhibits a CO_2 uptake of 0.41 g CO_2/g material after 20 cycles under CaL-CSP storage conditions, which is about the value reported by Obermeier et al. [42] for a synthetic composite with a molar ratio Ca/Al of 89/11 prepared by a more complex method such as liquid phase self-propagating high-temperature synthesis (LPSHS). Furthermore, our composite shows an enhanced performance compared to limestone when cycled under realistic CaL- CO_2 capture conditions (involving calcination at high CO_2 concentration and high temperature) whereas CaL conditions used in most of researches focused on Al-composites for CO_2 capture involve calcination under low CO_2 concentration atmospheres [58, 60].

3.2) Characterization of the composites after Ca-Looping cycles

3.2.1) X-Ray Diffraction

Figures 7-8 show the powder X-ray diffractograms of the different composites after being subjected to the CaL cycles under CaL-CSP storage and CO_2 capture conditions, respectively. In both cases, the presence of crystalline calcium aluminates is clearly appreciated. As expected, the diffraction peaks of the calcium aluminates become sharper and more intense as the alumina content is increased, which is especially marked for the 20wt Al_2O_3 composite under CO_2 capture conditions (Fig. 8). These calcium aluminates were formed from the first calcination.

A main observation from Figures 7-8 is that two distinct types of calcium aluminate are formed under the different CaL conditions tested. A cubic structure of $\text{Ca}_4(\text{Al}_2\text{O}_4)_3\text{O}$ has been identified as the crystalline aluminate formed under CaL-CSP storage conditions. As far as we know, this crystalline phase has not been reported before for Al-composites subjected to calcium looping cycles. On the other hand, the crystalline aluminate phase formed under CO_2 capture conditions correspond to $\text{Ca}_3\text{Al}_2\text{O}_6$, which is in agreement with the aluminate reported by others authors [33, 60]. The robustness of these results has been confirmed by using another limestone from a different quarry. The Ca/Al ratio of the irreversibly formed calcium

aluminates is therefore determined by the type of CaL conditions being it higher for CO₂ capture conditions, which withdraws a larger amount of active Ca for carbonation.

It is interesting to note the different size of the CaO crystallites after CaL-CSP storage and CaL-CO₂ capture multicycle tests (Table 3). The crystalline CaO generated from the calcination of the different samples under CaL-CO₂ capture conditions presents crystallite sizes about three times larger than that of those generated under CaL-CSP storage conditions. The explanation lies in the harsh calcination conditions utilized in CO₂ capture, high partial pressure of CO₂ and temperature, which promote CaO sintering and crystallite growth [50].

Table 3. CaO crystallite size (L (nm) estimated for the CaO reflection peak (200) at $2\theta = 37.4^\circ$) after the 20th cycle under CaL-CSP storage and CaL-CO₂ capture conditions. Estimated standard deviation for each value is included in parentheses.

	L (nm) Energy storage conditions	L (nm) CO ₂ capture conditions
0wt Al ₂ O ₃	37 (5)	53 (5)
5wt Al ₂ O ₃	17 (5)	64 (5)
10wt Al ₂ O ₃	21 (5)	60 (5)
20wt Al ₂ O ₃	22 (5)	57 (5)

The progressive formation of calcium aluminates as the number cycles increases occurs at different rates as depending of the CaL conditions employed. This has been checked in our work by preparing stoichiometric mixtures of CaCO₃ and Al₂O₃ (reactions (4) and (5), respectively) to produce the different kinds of calcium aluminates at CaL-CSP and CaL-CO₂ capture conditions,

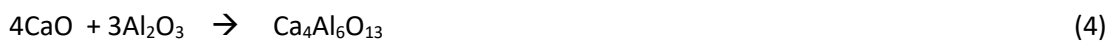
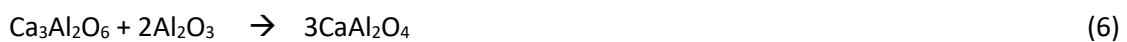


Figure 9 shows the X-ray diffractograms obtained after the 2nd calcination step under both types of CaL conditions. As may be seen, some CaO remains unreacted after calcination of the stoichiometric mixtures. However, it may be inferred from the peaks intensity that the amount of Ca₃Al₂O₆ formed after two calcination cycles under CaL-CO₂ capture conditions is much higher than the Ca₄Al₆O₁₃ amount formed under energy storage conditions. Additionally, CaAl₂O₄ is formed under CO₂ capture conditions in the stoichiometric mixture, following the reaction (6) [61]. Note that such crystalline phase was not observed in the composites tested (Figure 8).



The formation of a large quantity of calcium aluminate at CO₂ capture conditions in the first cycles would be favored by the high calcination temperature employed (900 °C). Thus, the formation of high amount of Ca₃Al₂O₆ at the beginning of the multicycle tests under CaL-CO₂

capture conditions could explain the relative variation of the effective conversion shown in Figure 6. Since most of the aluminates are formed from the first cycles, the relative variation of the effective conversion (Fig. 6) remains roughly constant along the cycles. On the other hand, $\text{Ca}_4\text{Al}_6\text{O}_{13}$ would be progressively formed with the number of cycles under CaL-CSP conditions, which would be related to the progressive increase observed for the relative variation of conversion (Fig. 6).

3.2.2) SEM microscopy

The samples cycled under energy storage and CO_2 capture conditions show evident morphological differences as seen in Figures 10 and 11, respectively. Such diverse CaL conditions produce on the CaO particles derived from limestone a well differentiated porous microstructure with pore sizes around 40 nm and 100 nm for CaL-CSP storage (Figure 10 a-c) and CO_2 capture (Figure 11 a-c) conditions, which is consistent with the observations reported in a previous work [39].

After the multicycle CaL tests at CaL-CSP storage conditions the surface of calcined milled limestone (0wt Al_2O_3) appears as a dense and cracked surface, with small grains and mesopores around 40 nm in size (Figure 10 a-c). Favorable conditions for carbonation in these tests (high CO_2 concentration and high temperature) lead to a quick built up of the CaCO_3 layer which, in addition to the relative small pore sizes generated during calcination (at the relatively low calcination temperature), hinders the CO_2 percolation into the inner grains of the CaO. This so-called pore plugging phenomenon is the limiting mechanism which is responsible for the activity loss under energy storage conditions as was shown in detail in previous works [23, 43]. After successive carbonation and calcinations, an external compact layer of CaO is generated, as observed in the corresponding micrographs (Fig. 10 a-c). In contrast, the calcined Al-composites after the cycles show a more porous and less sintered surface morphology. The calcined 5wt Al_2O_3 composite exhibit the least sintered particles, with macropores and cavities of size between 0.5 and 2 μm (Figure 10d). On the other hand, the surface of the calcined 20wt Al_2O_3 composite shows a higher proportion of nanoparticles and a marked decrease in the macropore size (Figure 10j). Modification of the pore size distributions through alumina addition could explain the different multicycle behavior of the different Al-composites. Thus, a lower proportion of alumina generates and preserves enough large pores during the CaL-CSP multicycle process, which inhibits pore-plugging as the formation of narrow pores is minimized. This observation could explain the higher effective conversion of the 5wt Al_2O_3 composite shown in Figure 4. A further beneficial effect of using less Al content is that less CaO is irreversible withdrawn to form calcium aluminates.

As seen in Figure 11, under CaL- CO_2 capture conditions, the addition of nanoalumina results in a large proportion of grains smaller than 500 nm as compared to the same sample after being subjected to CaL-CSP storage conditions (compare Figure 11i and Figure 10i for example). Furthermore, these small grains seem to block the pores of the CaO particles, which is more pronounced as the content of alumina is increased as clearly seen for the 20wt Al_2O_3 composite (Figure 11l). Moreover, the tortuous pore structure shown by this sample could hinder the diffusion of the CO_2 to the active sites within the particles. The importance of the

morphology and porosity of the sorbent for CO₂ capture has been already pointed out by other authors [25, 58, 62-64]. The loss of surface area and therefore capture capacity has been attributed to morphological changes due to the formation of calcium aluminates and sintering effects [40]. Many studies have evidenced that the CO₂ uptake of a sorbent is enhanced by large surface area values [52, 65], albeit it is influenced also by the pore network and tortuosity [58, 66].

3.2.3) HRTEM microscopy

Al-composites are characterized by two different nanostructure types as evidenced by the HRTEM micrographs in Fig. 12. Some of the CaO particles are formed by small grains of CaO ranging from 20 to 50 nm (Fig.12 a, b) whereas others are characterized by a smooth and uniform surface (Fig.12 c, d) showing a high Al content associated to calcium aluminate as revealed by the compositional mapping (Figure 13). The size of the calcium aluminate particles is on the order of few nanometers up to 500 nm being found mainly at the periphery of the micrometric CaO particles of the composites as shown in Figures 13 and 14. This type of arrangement has not been clearly evidenced in previous works to our knowledge. Presumably, the steric hindrance of the formed calcium aluminates would mitigate sintering of the CaO grains along the CaL cycles, which might explain the observed enhancement of activity, especially under energy storage conditions. However, this steric hindrance could not be efficient enough to avoid the deactivation process of Al-composites under CaL-CO₂ capture conditions.

A HAADF-STEM mapping analysis of the distinct aluminate grains shows their different compositions as depending on the type of conditions either CaL-CSP storage (Figure 15) or CaL-CO₂ capture (Figure 16) conditions. The atomic ratio Ca/Al of the aluminate generated under CaL-CSP storage conditions is close to 0.67, which is consistent with the ratio of the Ca₄(Al₂O₄)₃O observed from X-ray diffraction (Fig. 7). In contrast, the Ca/Al ratio of the aluminate obtained under CO₂ capture conditions is significantly higher and close to Ca/Al = 1.5, which matches the tricalcium aluminate Ca₃Al₂O₆ revealed by the XRD analysis (Fig. 8). Thus, the formation of Ca₃Al₂O₆ consumes a higher amount of available CaO as compared to Ca₄(Al₂O₄)₃O which could explain the low activity of the composite 20wt Al₂O₃ under CO₂ capture conditions, as observed in Figure 4.

The formation of diverse calcium aluminate binders and microstructures under CaL-CSP storage and CaL-CO₂ capture conditions explains the different behavior of the Al-composites prepared in the present work as depending on the CaL conditions used. The simple milling pretreatment proposed could be economically viable for synthesizing large quantities of enhanced CaO-based sorbents as demonstrated by our results. However, a detailed study on the fluidization behavior of these composites and pellets obtained from them for their practical use in fluidized beds and cyclonic separators must be addressed in future works. Certainly, the particles used in our study are too small to be used in circulating fluidized beds, where optimum particle size is on the order of 100 μm [5]. For that purpose, pelletization of the milled powders would be required. We note however that the formation of calcium aluminates is expected to mitigate pore plugging as main limiting mechanism for the

multicycle activity at CaL conditions for energy storage [43]. At CO₂ capture conditions, sintering as main limiting mechanism does not pose a constraint to particle size in this range [53, 67, 68].

4. Conclusions

This work is focused on the Calcium Looping performance of Al₂O₃/CaO composites synthesized by mechanical milling of nanoalumina/limestone mixtures. It has been found that these composites exhibit different behaviors as depending on the type of CaL application, either for energy storage in CSP or for CO₂ capture, which has not been reported in previous works. The CaL performance of the composites can be rationalized from the diverse types of microstructure generated under CaL-CSP and CaL-CO₂ capture conditions due to the different carbonation and calcination conditions. Thus, calcination is carried out at high temperatures (>900 °C) under high CO₂ concentration in the CO₂ capture application whereas it is performed at relatively moderate temperature (~ 700 °C) under an inert gas for CSP energy storage. On the other hand, carbonation in the CO₂ capture application takes place at ~650 °C under a 15%vol CO₂ concentration environment whereas it occurs at relatively high temperature (~850 °C) under a high CO₂ concentration atmosphere for CSP energy storage. The formation of two distinct types of calcium aluminate as depending on the type of CaL conditions affects distinctly the microstructure and morphology of the CaO grains due to the steric hindrance effects of the aluminates. Thus, a calcium aluminate with ratio Ca/Al < 1 is formed under CaL-CSP storage conditions, which stabilizes the CaO microstructure and serves to mitigate pore-plugging as the main limiting mechanism under these conditions. Under CaL-CSP storage conditions, the residual effective conversion values are similar for the different Al-composites tested regardless of the Al₂O₃ content (in the range 5wt% to 20 wt%, $X_{ef,r} \sim 0.35$) and well above the residual conversion obtained for the limestone milled without additive ($X_{ef,r} = 0.16$). On the other hand, under CaL-CO₂ capture conditions, the crystalline phase Ca₃Al₂O₆ generated leads to a higher consumption of the CaO available, which yields a severe drop of the multicycle activity for the composites with larger than 5wt% Alumina. Only the composite with low Al₂O₃ content (5 wt%) yields a residual effective conversion value ($X_{ef,r} = 0.097$) higher than that obtained for the milled limestone ($X_{ef,r} = 0.082$). Therefore, it can be concluded that the 5wt% Al₂O₃ milled composite exhibits the best performance for prolonged cycles tests under both type of CaL conditions applied to CSP storage and CO₂ capture.

Acknowledgments

This work has been supported by the Spanish Government Agency Ministerio de Economía y Competitividad (MINECO-FEDER funds, contracts CTQ2014-52763-C2, CTQ2017-83602-C2). AP thanks financial support from VI PPIT-US and VPPI-US for his current contract. We acknowledge the Functional Characterization services of Innovation, Technology and

Research Center of the University of Seville (CITIUS) and the characterization services of the Institute of Materials Science of Seville (ICMS).

References

- [1] S. Chu, A. Majumdar, Opportunities and challenges for a sustainable energy future, *Nature* 488 (2012) 294-303.
- [2] B. Arias, M.E. Diego, J.C. Abanades, M. Lorenzo, L. Diaz, D. Martínez, J. Alvarez, A. Sánchez-Biezma, Demonstration of steady state CO₂ capture in a 1.7 MWth calcium looping pilot, *Int. J. Greenh. Gas Control* 18 (2013) 237-245.
- [3] M.H. Chang, C.M. Huang, W.H. Liu, W.C. Chen, J.Y. Cheng, W. Chen, T.W. Wen, S. Ouyang, C.H. Shen, H.W. Hsu, Design and experimental investigation of Calcium Looping Process for 3-kWth and 1.9-MWth Facilities, *Chem. Eng. Technol.* 36 (2013) 1525-1532.
- [4] J. Ströhle, M. Junk, J. Kremer, A. Galloy, B. Epple, Carbonate looping experiments in a 1 MWth pilot plant and model validation, *Fuel* 127 (2014) 13-22.
- [5] D.P. Hanak, E.J. Anthony, V. Manovic, A review of developments in pilot-plant testing and modelling of calcium looping process for CO₂ capture from power generation systems, *Energy Environ. Sci.* 8 (2015) 2199-2249.
- [6] J. Blamey, E.J. Anthony, J. Wang, P.S. Fennell, The calcium looping cycle for large-scale CO₂ capture, *Prog. Energy Combust. Sci.* 36 (2010) 260-279.
- [7] A. Perejón, L.M. Romeo, Y. Lara, P. Lisbona, A. Martínez, J.M. Valverde, The Calcium-Looping technology for CO₂ capture: On the important roles of energy integration and sorbent behavior, *Appl. Energy* 162 (2016) 787-807.
- [8] K.E. N'Tsoukpoe, H. Liu, N. Le Pierrès, L. Luo, A review on long-term sorption solar energy storage, *Renew. Sust. Energ. Rev.* 13 (2009) 2385-2396.
- [9] P. Pardo, A. Deydier, Z. Anxionnaz-Minvielle, S. Rougé, M. Cabassud, P. Cognet, A review on high temperature thermochemical heat energy storage, *Renew. Sust. Energ. Rev.* 32 (2014) 591-610.
- [10] C. Prieto, P. Cooper, A.I. Fernández, L.F. Cabeza, Review of technology: Thermochemical energy storage for concentrated solar power plants, *Renew. Sust. Energ. Rev.* 60 (2016) 909-929.
- [11] C. Tregambi, P. Salatino, R. Solimene, F. Montagnaro, An experimental characterization of Calcium Looping integrated with concentrated solar power, *Chem. Eng. J.* 331 (2018) 794-802.
- [12] K. Kyaw, H. Matsuda, M. Hasatani, Applicability of carbonation/decarbonation reactions to high-temperature thermal energy storage and temperature upgrading, *J. Chem. Eng. Jpn.* 29 (1996) 119-125.
- [13] R. Chacartegui, A. Alovisio, C. Ortiz, J.M. Valverde, V. Verda, J.A. Becerra, Thermochemical energy storage of concentrated solar power by integration of the calcium looping process and a CO₂ power cycle, *Appl. Energy* 173 (2016) 589-605.
- [14] S.E.B. Edwards, V. Materić, Calcium looping in solar power generation plants, *Sol. Energy* 86 (2012) 2494-2503.
- [15] B. Sarrion, J.M. Valverde, A. Perejon, L. Perez-Maqueda, P.E. Sanchez-Jimenez, On the multicycle activity of natural limestone/dolomite for thermochemical energy storage of concentrated solar power, *Energy Technol.* 4 (2016) 1013-1019.
- [16] E.E. Berger, Effect of steam on the decomposition of limestone 1,1, *Ind. Eng. Chem.* 19 (1927) 594-596.
- [17] E.L. Cussler, *Diffusion: Mass Transfer in Fluid Systems*, Cambridge University Press, 1997.
- [18] E. Taketomo, M. Fujiura, Porous materials for concentration and separation of hydrogen or helium, and process therewith for the separation of the gas, US patent 4482360, 1984.

- [19] M. Erans, V. Manovic, E.J. Anthony, Calcium looping sorbents for CO₂ capture, *Appl. Energy* 180 (2016) 722-742.
- [20] A.M. Kierzkowska, R. Pacciani, C.R. Müller, CaO-Based CO₂ sorbents: From fundamentals to the development of new, highly effective materials, *ChemSusChem* 6 (2013) 1130-1148.
- [21] J.M. Valverde, Ca-based synthetic materials with enhanced CO₂ capture efficiency, *J. Mater. Chem. A* 1 (2013) 447-468.
- [22] K.G. Sakellariou, G. Karagiannakis, Y.A. Criado, A.G. Konstandopoulos, Calcium oxide based materials for thermochemical heat storage in concentrated solar power plants, *Sol. Energy* 122 (2015) 215-230.
- [23] M. Benitez-Guerrero, J.M. Valverde, P.E. Sanchez-Jimenez, A. Perejon, L.A. Perez-Maqueda, Multicycle activity of natural CaCO₃ minerals for thermochemical energy storage in Concentrated Solar Power plants, *Sol. Energy* 153 (2017) 188-199.
- [24] B.R. Stanmore, P. Gilot, Review—calcination and carbonation of limestone during thermal cycling for CO₂ sequestration, *Fuel Process. Technol.* 86 (2005) 1707-1743.
- [25] P. Sun, J.R. Grace, C.J. Lim, E.J. Anthony, The effect of CaO sintering on cyclic CO₂ capture in energy systems, *AIChE Journal* 53 (2007) 2432-2442.
- [26] V. Manovic, E.J. Anthony, Thermal activation of CaO-based sorbent and self-activation during CO₂ capture looping cycles, *Environ. Sci. Technol.* 42 (2008) 4170-4174.
- [27] J.M. Valverde, P.E. Sanchez-Jimenez, L.A. Perez-Maqueda, Effect of heat pretreatment/recarbonation in the Ca-looping process at realistic calcination conditions, *Energy Fuels* 28 (2014) 4062-4067.
- [28] J.M. Valverde, P.E. Sanchez-Jimenez, L.A. Perez-Maqueda, Role of precalcination and regeneration conditions on postcombustion CO₂ capture in the Ca-looping technology, *Appl. Energy* 136 (2014) 347-356.
- [29] J.M. Valverde, M. Barea-López, A. Perejón, P.E. Sanchez-Jimenez, L.A. Perez-Maqueda, Thermochemical energy storage for concentrated solar power using natural limestone: Thermal pretreatment and nanosilica addition, *Energy Fuels* 31 (2017) 4226-4236.
- [30] V. Manovic, E.J. Anthony, Steam reactivation of spent CaO-based sorbent for multiple CO₂ capture cycles, *Environ. Sci. Technol.* 41 (2007) 1420-1425.
- [31] P. Sun, J.R. Grace, C.J. Lim, E.J. Anthony, Investigation of attempts to improve cyclic CO₂ capture by sorbent hydration and modification, *Ind. Eng. Chem. Res.* 47 (2008) 2024-2032.
- [32] M. Sayyah, Y. Lu, R.I. Masel, K.S. Suslick, Mechanical activation of CaO-based adsorbents for CO₂ capture, *ChemSusChem* 6 (2013) 193-198.
- [33] J. Sun, W. Liu, M. Li, X. Yang, W. Wang, Y. Hu, H. Chen, X. Li, M. Xu, Mechanical modification of naturally occurring limestone for high-temperature CO₂ capture, *Energy Fuels* 30 (2016) 6597-6605.
- [34] P.E. Sanchez-Jimenez, J.M. Valverde, A. Perejón, A. de la Calle, S. Medina, L.A. Pérez-Maqueda, Influence of ball milling on CaO crystal growth during limestone and dolomite calcination: Effect on CO₂ capture at Calcium Looping conditions, *Cryst. Growth Des.* 16 (2016) 7025-7036.
- [35] M. Broda, A.M. Kierzkowska, C.R. Müller, Influence of the calcination and carbonation conditions on the CO₂ uptake of synthetic Ca-based CO₂ sorbents, *Environ. Sci. Technol.* 46 (2012) 10849-10856.
- [36] S.F. Wu, Q.H. Li, J.N. Kim, K.B. Yi, Properties of a nano CaO/Al₂O₃ CO₂ sorbent, *Ind. Eng. Chem. Res.* 47 (2008) 180-184.
- [37] M. Broda, A.M. Kierzkowska, C.R. Müller, Application of the sol-gel technique to develop synthetic calcium-based sorbents with excellent carbon dioxide capture characteristics, *ChemSusChem* 5 (2012) 411-418.
- [38] C. Qin, W. Liu, H. An, J. Yin, B. Feng, Fabrication of CaO-based sorbents for CO₂ capture by a mixing method, *Environ. Sci. Technol.* 46 (2012) 1932-1939.
- [39] S. Stendardo, L.K. Andersen, C. Herce, Self-activation and effect of regeneration conditions in CO₂-carbonate looping with CaO-Ca₁₂Al₁₄O₃₃ sorbent, *Chem. Eng. J.* 220 (2013) 383-394.

- [40] N.H. Florin, J. Blamey, P.S. Fennell, Synthetic CaO-based sorbent for CO₂ capture from large-point sources, *Energy Fuels* 24 (2010) 4598-4604.
- [41] K.G. Sakellariou, N.I. Tsongidis, G. Karagiannakis, A.G. Konstandopoulos, D. Baciú, G. Charalambopoulou, T. Steriotis, A. Stubos, W. Arlt, Development and evaluation of materials for thermochemical heat storage based on the CaO/CaCO₃ reaction couple, *AIP Conference Proceedings* 1734 (2016) 050040.
- [42] J. Obermeier, K.G. Sakellariou, N.I. Tsongidis, D. Baciú, G. Charalambopoulou, T. Steriotis, K. Müller, G. Karagiannakis, A.G. Konstandopoulos, A. Stubos, W. Arlt, Material development and assessment of an energy storage concept based on the CaO-looping process, *Sol. Energy* 150 (2017) 298-309.
- [43] M. Benitez-Guerrero, B. Sarrion, A. Perejon, P.E. Sanchez-Jimenez, L.A. Perez-Maqueda, J.M. Valverde, Large-scale high-temperature solar energy storage using natural minerals, *Sol. Energy Mater. Sol. Cells* 168 (2017) 14-21.
- [44] S. Brunauer, P.H. Emmett, E. Teller, Adsorption of gases in multimolecular layers, *J. Am. Chem. Soc.* 60 (1938) 309-319.
- [45] H. Choi, W. Lee, S. Kim, Effect of grinding aids on the kinetics of fine grinding energy consumed of calcite powders by a stirred ball mill, *Adv. Powder Technol.* 20 (2009) 350-354.
- [46] M. Sayyah, Calcium oxide-based sorbents for CO₂ capture at high temperature, Ph.D. Thesis, University of Illinois at Urbana-Champaign, United States, Illinois, 2013.
- [47] G.S. Grasa, J.C. Abanades, CO₂ capture capacity of CaO in long Series of carbonation/calcination cycles, *Ind. Eng. Chem. Res.* 45 (2006) 8846-8851.
- [48] J.M. Valverde, A model on the CaO multicyclic conversion in the Ca-looping process, *Chem. Eng. J.* 228 (2013) 1195-1206.
- [49] J.M. Valverde, P.E. Sanchez-Jimenez, A. Perejon, L.A. Perez-Maqueda, CO₂ multicyclic capture of pretreated/doped CaO in the Ca-Looping process. Theory and experiments, *Phys. Chem. Chem. Phys.* 15 (2013) 11775-11793.
- [50] J.M. Valverde, P.E. Sanchez-Jimenez, L.A. Perez-Maqueda, Limestone calcination nearby equilibrium: Kinetics, CaO crystal structure, sintering and reactivity, *J. Phys. Chem. C* 119 (2015) 1623-1641.
- [51] Y. Liu, Y. Yang, Evolution of the surface area of limestone during calcination and sintering, *J. Power Energy Eng.* 3 (2015) 56-62.
- [52] R. Barker, The reversibility of the reaction $\text{CaCO}_3 \rightleftharpoons \text{CaO} + \text{CO}_2$, *J. Appl. Chem. Biotechnol.* 23 (1973) 733-742.
- [53] G. Grasa, R. Murillo, M. Alonso, J.C. Abanades, Application of the random pore model to the carbonation cyclic reaction, *AIChE J.* 55 (2009) 1246-1255.
- [54] S.K. Bhatia, D.D. Perlmutter, Effect of the product layer on the kinetics of the CO₂-lime reaction, *AIChE J.* 29 (1983) 79-86.
- [55] Z. Sun, S. Luo, P. Qi, L.-S. Fan, Ionic diffusion through Calcite (CaCO₃) layer during the reaction of CaO and CO₂, *Chem. Eng. Sci.* 81 (2012) 164-168.
- [56] Z.-s. Li, F. Fang, X.-y. Tang, N.-s. Cai, Effect of temperature on the carbonation reaction of CaO with CO₂, *Energy Fuels* 26 (2012) 2473-2482.
- [57] C. Ortiz, J.M. Valverde, R. Chacartegui, Energy consumption for CO₂ capture by means of the Calcium Looping process: A Comparative Analysis using Limestone, Dolomite, and Steel Slag, *Energy Technol.* 4 (2016) 1317-1327.
- [58] D. Karami, N. Mahinpey, Study of Al₂O₃ addition to synthetic Ca-based sorbents for CO₂ sorption capacity and stability in cyclic operations, *The Canadian Journal of Chemical Engineering* 93 (2015) 102-110.
- [59] J.-y. Jing, T.-y. Li, X.-w. Zhang, S.-d. Wang, J. Feng, W.A. Turmel, W.-y. Li, Enhanced CO₂ sorption performance of CaO/Ca₃Al₂O₆ sorbents and its sintering-resistance mechanism, *Appl. Energy* 199 (2017) 225-233.
- [60] Y. Li, L. Shi, C. Liu, Z. He, S. Wu, Studies on CO₂ uptake by CaO/Ca₃Al₂O₆ sorbent in calciums looping cycles, *J. Thermal Anal. Calorim.* 120 (2015) 1519-1528.

- [61] Y. Tian, X. Pan, H. Yu, G. Tu, Formation mechanism of calcium aluminate compounds based on high-temperature solid-state reaction, *J. Alloy. Compd.* 670 (2016) 96-104.
- [62] P.S. Fennell, R. Pacciani, J.S. Dennis, J.F. Davidson, A.N. Hayhurst, The Effects of Repeated Cycles of Calcination and Carbonation on a Variety of Different Limestones, as Measured in a Hot Fluidized Bed of Sand, *Energy Fuels* 21 (2007) 2072-2081.
- [63] H. Lu, A. Khan, P.G. Smirniotis, Relationship between Structural Properties and CO₂ Capture Performance of CaO-Based Sorbents Obtained from Different Organometallic Precursors, *Ind. Eng. Chem. Res.* 47 (2008) 6216-6220.
- [64] Y. Li, C. Zhao, H. Chen, Y. Liu, Enhancement of Ca-based sorbent multicyclic behavior in Ca looping process for CO₂ separation, *Chem. Eng. Technol.* 32 (2009) 548-555.
- [65] R. Filitz, A.M. Kierzkowska, M. Broda, C.R. Müller, Highly efficient CO₂ sorbents: Development of synthetic, calcium-rich dolomites, *Environ. Sci. Technol.* 46 (2012) 559-565.
- [66] C.S. Martavaltzi, A.A. Lemonidou, Development of new CaO based sorbent materials for CO₂ removal at high temperature, *Microporous Mesoporous Mat.* 110 (2008) 119-127.
- [67] J.C. Abanades, D. Alvarez, Conversion limits in the reaction of CO₂ with lime, *Energy Fuels* 17 (2003) 308-315.
- [68] I. Martinez, G. Grasa, R. Murillo, B. Arias, J.C. Abanades, Kinetics of Calcination of Partially Carbonated Particles in a Ca-Looping System for CO₂ Capture, *Energy Fuels* 26 (2012) 1432 - 1440.